An integrated approach to mixing sensitivities in tropospheric chemistry: A basis for the parameterization of subgrid-scale emissions for chemistry transport models

J. G. Esler

Department of Mathematics, University College London, UK

Received 23 March 2003; revised 23 May 2003; accepted 8 July 2003; published 18 October 2003.

[1] The net effect on the global atmosphere of a continuous isolated chemical source is considered under idealized conditions. A general framework is described that allows M_i, the steady state global perturbation to the ith species due to the source, to be calculated. This is achieved by exploiting the fact that once the emissions are sufficiently dilute, far from the source, they decay with the timescales of the chemical eigenstates of the background atmosphere. Both M_i and the level of excitation of the longer-lived eigenstates are shown to depend on the details of the mixing of emissions near the source. If the details of the dilution of the emissions plume are known, it is also shown that ''equivalent emissions'' can be calculated. Equivalent emissions are designed so that when diluted instantaneously into the background atmosphere they result in the same global perturbation to each species as the original slowly diluted plume. The framework is then applied to test the sensitivity to mixing of a simple O_3-NO_x-CO-HO_x tropospheric chemistry system. M_i is calculated for a NO-CO source of constant strength as the mixing scenario undergone by the emissions is varied. The global increase in O_3 due to the source is found to increase with the rate at which emissions are mixed, whereas the global increase in CO is reduced. The equivalent emissions for each plume dilution mechanism are then calculated. In a simple plume box model it is shown that the equilibrium state obtained when the model is forced by emissions that are first diluted in entraining plumes can be reproduced in a standard box model (i.e., with instantaneous mixing of emissions) by the corresponding equivalent emissions. It is argued that the concept of equivalent emissions can be exploited straightforwardly to derive a parameterization of unresolved subgrid plumes in order to reduce systematic error in global models. *INDEX TERMS:* 0343 Atmospheric Composition and Structure: Planetary atmospheres (5405, 5407, 5409, 5704, 5705, 5707); 0365 Atmospheric Composition and Structure: Troposphere—composition and chemistry; 0368 Atmospheric Composition and Structure: Troposphere—constituent transport and chemistry; *KEYWORDS:* tropospheric chemistry, mixing sensitivity, emissions parameterization

Citation: Esler, J. G., An integrated approach to mixing sensitivities in tropospheric chemistry: A basis for the parameterization of subgrid-scale emissions for chemistry transport models, *J. Geophys. Res.*, *108*(D20), 4632, doi:10.1029/2003JD003627, 2003.

1. Introduction

[2] It is widely recognized that nonlinearity in atmospheric chemistry causes global-scale chemical distributions to be sensitive to mixing processes. For example, the rate and total amount of ozone loss in the lower stratosphere in Northern springtime are both sensitive to the rate of mixing between vortex air and midlatitude air [*Eduoard et al.*, 1996a, 1996b; *Tan et al.*, 1998]. Similarly *Esler et al.* [2001] have found that hydroxyl radical (OH) concentrations are sensitive to mixing between tropospheric and stratospheric air during stratosphere-troposphere exchange events, with implications for the oxidizing capacity of the troposphere. Mixing sensitivities of this type raise the question: how much effort is required toward understanding and modeling atmospheric mixing processes in order to accurately model global atmospheric chemistry? To begin to answer this question, the sensitivity to mixing of a simple model of tropospheric chemistry is described below, together with a framework for quantitatively assessing the impact on global chemical budgets of different mixing scenarios for tropospheric emissions.

[3] In the troposphere many important reactions involve radical species including HO_x (= OH + HO_2, the hydroperoxy radical). The behavior of these species during mixing processes is central to understanding mixing sensitivities in the troposphere. On timescales longer than their chemical lifetimes (typically <1 min for OH, 10–15 mins for HO_x), HO_x radicals are not conserved under mixing processes. This is because they adjust to a photochemical equilibrium state [*Ehhalt*, 1998] that depends nonlinearly

0148-0227/03/2003JD003627

on the local concentrations of longer-lived precursor species (e.g., nitrogen oxides NO_x = NO + NO_2, carbon monoxide CO and ozone O_3). The total mass of each precursor is conserved when two air masses mix, but because mixing can change local concentrations, it can lead to systematic changes not only to the local HO_x concentrations but also to the total mass of OH and HO_2 and other radical species. The sensitivity of HO_x to NO_x concentrations in particular [*Kley*, 1997; *Faloona et al.*, 2000] means that there is particularly strong sensitivity to mixing near sources of NO_x.

[4] A related sensitivity to mixing in the troposphere concerns the amount of secondary ozone production, due to emissions of NO_x, in the cycle:

$$\begin{aligned} &\mathrm{NO} + \mathrm{HO_2} \rightarrow \mathrm{NO_2} + \mathrm{OH} \\ &\mathrm{NO_2} + h\nu \rightarrow \mathrm{NO} + \mathrm{O} \\ &\mathrm{O} + \mathrm{O_2} \rightarrow \mathrm{O_3} \\ \text{net}: \quad &\mathrm{O_2} + \mathrm{HO_2} \rightarrow \mathrm{O_3} + \mathrm{OH}. \end{aligned}$$

The ratio of ozone molecules produced to NO_x molecules emitted, ϵ_N, is thought to increase with the rate of mixing of the NO_x emissions [*Lin et al.*, 1988; *Chatfield and Delaney*, 1990; *Liang and Jacobson*, 2000]. Consequently *Jacob et al.* [1993] argued that ϵ_N is greater in the western United States in summer compared with the east because in the west boundary layer conditions lead to more rapid mixing. *Wild et al.* [1996] and *Poppe et al.* [1998] have investigated this issue in idealized models by comparing the concentrations of ozone and other species within a polluted plume undergoing dilution at various rates. The former study noted that, unsurprisingly, ozone concentration were lower the more rapidly the polluted plume was diluted by background air. However, *Poppe et al.* [1998] pointed out that the maximum amount of anomalous ozone integrated across the plume at certain times was usually greater when the plume was diluted rapidly, despite the concentrations in the plume being lower.

[5] The novel approach here is that the ''integrated'' effects of different mixing scenarios for emissions are considered. When a relatively short-lived species (e.g., NO) is released into the troposphere it is now widely recognized that the resulting (globally integrated) chemical perturbation may persist for a much longer timescale than either the chemical lifetime of the species (the lifetime of NO_x is several days) or the timescale on which observable chemical anomalies from the emission are uniformly mixed into the tropospheric background (days to weeks depending on the initial scale of the emission and meteorological conditions). The globally integrated chemical anomaly persists because the released NO indirectly excites perturbations in longer-lived species (e.g., O_3, CO, CH_4) that will eventually decay on the timescale of the longest-lived tropospheric chemical eigenstate ($\sim$14 years) [*Prather*, 1994; *Wild et al.*, 2001]. If the global warming potential, or total impact on tropospheric oxidizing capacity, of a given emission is to be evaluated, it is therefore necessary to consider its integrated effect as opposed to merely the short-time, directly observable response in trace gas concentrations near the source. This paper uses a simplified framework to determine the extent to which the mixing scenario experienced by an emission near its source can affect the resulting long-time decay of the chemical perturbation, i.e., the level of excitation of the longer-lived eigenstates. Not only is the overall integrated response to an emission found to be sensitive to the initial mixing near the source, but this sensitivity is shown to depend just as much on changes in the long-time behavior as on changes to the more immediate, directly observable, response discussed by *Poppe et al.* [1998] and the other references above.

[6] The framework developed to address the above issues is then exploited to outline a methodology for parameterizing subgrid scale emissions in chemistry transport models (CTMs). In CTMs it is not possible to resolve each individual chemical source and therefore emissions are generally diluted directly into model grid-boxes. Even in high resolution models this represents unphysical rapid mixing which is subsequently artificially enhanced by numerical diffusion. As a result systematic errors are introduced [*Pyle and Zavody*, 1990], which, due to the coupled nature of the chemistry will affect the concentration of many important species. In the suggested parameterization subgrid emissions are replaced by ''equivalent emissions'' that depend on the (known) details of the dilution of the subgrid plume as well as the subgrid emissions themselves. The equivalent emissions are designed so that when diluted instantly into a CTM model grid-box they result in the same global perturbation to each species that the subgrid emissions would cause if the plume in which they were diluted were perfectly resolved. Further, the equivalent emissions converge to the same long-time decaying chemical perturbation as the products from the subgrid plume.

[7] The potential advantages of using equivalent emissions to parameterize subgrid sources in global CTMs include the fact the computational costs are entirely off line. Previous attempts using nested grid-boxes for the sources [*Sillman et al.*, 1990; *Jacob et al.*, 1993] were not only computationally expensive but also allowed only a discrete resolution of the plumes and a small number of possible source concentrations. The equivalent emissions are also well-defined for any given plume, so that the type of problem encountered by some current parameterizations of aircraft emissions [*Kraabøl et al.*, 2000; *Meijer*, 2001] where some of the chemical products in the plume are arbitrarily discarded from treatment in the model, are eliminated.

[8] In section 2 below we develop the general integrated framework which allows the global influence of emissions from an individual source to be shown explicitly to be a function of the mixing scenario of the emissions. In section 2.2 we show that this framework allows us to calculate equivalent emissions satisfying the desirable properties detailed above. In section 3 we describe a reduced tropospheric chemistry in which HO_x concentrations are explicitly determined from their precursor concentrations using photochemical steady state expressions. Section 4 contains the results of a study using this chemistry scheme where the total global perturbation due to an emissions site is evaluated under different mixing conditions. Equivalent

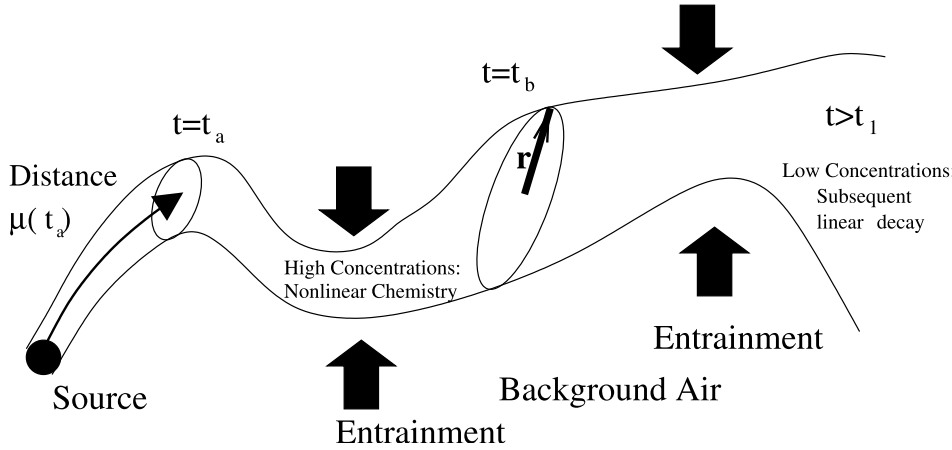

Figure 1. Schematic showing a plume downstream of a chemical source. The time t since emission is taken as the along-plume coordinate, and the cross-sectional coordinate system is illustrated by the vector **r**. At early times after emission (e.g., t_a, t_b shown), nonlinear chemistry in the plume requires equation (2) to be solved explicitly. However, at later times ($t \geq t_1$) the plume is dilute and the subsequent decay of the emissions can be approximated by equation (7).

emissions are then calculated for each type of plume considered. In section 5 we consider an idealized model problem. When a global box model forced by many entraining plumes is compared to a standard box model forced by equivalent emissions, it is shown that the mean equilibrium concentrations of each species can be reproduced. Section 6 contains our conclusions.

2. Sensitivity to Mixing and Equivalent Emissions: Theory

2.1. A Framework for Assessing Globally Integrated Sensitivity to Mixing

[9] A useful starting point for understanding chemistry-mixing interactions in the troposphere is to consider the effect of a single emissions site or chemical source on a effectively infinite background atmosphere. This approach has been used in previous studies of chemistry-mixing interaction [*Wild et al.*, 1996; *Poppe et al.*, 1998]. In these studies a mixing scenario for the emissions was postulated and results for different entrainment rates were compared at selected times after emission from the source. An alternative approach, using multiple box models, compares the net chemical effects of ''instantaneous mixing'' between air masses to ''no mixing'' between air masses [*Liang and Jacobson*, 2000; *Esler et al.*, 2001]. Although the results of these studies broadly agree that more rapid mixing of high NO_x air masses leads to more efficient ozone production (except in isolated examples discussed by *Poppe et al.* [1998]), the necessity of selecting comparison times means that it is difficult to compare results quantitatively. This is especially true when comparing qualitatively different mixing scenarios for the emissions. Also, the effect of the initial mixing scenario on the long-time decay of the chemical perturbation, after the initial emissions are both widely dispersed and very dilute, was not considered by any of the above studies. In this section we aim to improve on this situation by introducing a framework where the global impact of a single source can be considered as a function of the mixing scenario of the emissions from that source. In particular this framework elucidates how the initial mixing can influence the long-time decay of the chemical products once they are diluted into the background.

[10] The background atmosphere can be considered to be ''infinite'' with respect to a single source if the contribution of that source to the global budget of each trace gas is small, in a sense to be discussed below. Provided that the chemistry under consideration is far from those parameter regimes exhibiting excitable chaotic behavior (as considered by, e.g., *Hess and Madronich* [1997]), as will be ensured if all the chemical Lyapunov exponents [*Neufeld et al.*, 1999] are negative, an isolated chemical source will lead to a perturbation that decays exponentially at long times. The source will therefore cause only a finite perturbation to the background atmosphere. We can therefore ask the following question: How does the total anomaly of each trace gas due to a single point source depend on the way those emissions are mixed into the background?

[11] Consider a chemical system of N species where the mixing ratio of each species X_i evolves according to

$$\frac{dX_i}{dt} = S_i + f_i(X_1, .., X_N) - k\nabla^2 X_i, \qquad i = 1, .., N. \qquad (1)$$

Here the operator d/dt is the usual advective derivative following the fluid velocity, S_i represents the spatially localized source of the ith species, and f_i is the chemistry acting on the ith species and k is the diffusivity. The combined effects of fluid dynamical stirring and mixing by diffusion eventually cause emissions far from the source to become dilute, i.e., with low concentrations spread over a large volume.

[12] Figure 1 illustrates the situation near a source region, such as a surface industrial site or aircraft engine. For the purposes of this paper, we shall assume that emissions evolve in continuous (turbulent) plumes stretching downstream from each source as illustrated. Selecting one such isolated source we denote the source of the ith species by δS_i. In the plume, the anomalous chemical concentration of

the ith species is denoted by $\delta X_i(t, \mathbf{r})$, so that in the plume the concentration satisfies $X_i = X_i^B + \delta X_i$ where X_i^B is the background concentration. In this plume equation t is the (mean) time since emission of the chemicals in the plume, and therefore also has a role as an along-plume coordinate. The single-valued function $\mu(t)$ is defined to be the distance along the plume, i.e., it assumed that at a time t after emission the chemicals have been advected a distance μ from the source. Finally, the vector $\mathbf{r}$ denotes the cross-sectional position in the plume. The plume may entrain and mix with background air as t increases, until at some time t_1, δX_i is small everywhere and the plume may be considered to be dilute.

[13] Considering the chemistry in the presence and in the absence of the source, δX_i evolves according to

$$\frac{d\,\delta X_i}{dt} = \delta S_i + f_i\left(X_1^B + \delta X_1, .., X_N^B + \delta X_N\right) - f_i\left(X_1^B, .., X_N^B\right) - k\nabla^2\,\delta X_i, \qquad i = 1, .., N. \tag{2}$$

The total amount of chemical products in the plume at time t after release can be written as an integral over a volume element δV of the plume. We shall denote this integral by an overbar,

$$\overline{\delta X_i}(t) = \int_A \delta X_i(t, \mathbf{r})\frac{d\mu}{dt}\,dA \qquad i = 1, .., N, \tag{3}$$

where A is the cross-sectional area of the plume. The volume element $\delta V(t) = A(t)d\mu/dt$ has units of volume per unit time and is conserved in the absence of entrainment. Note, however, that $d\mu/dt$, the rate of increase of distance from the source with time from emission, and the cross-sectional area $A(t)$ can change as chemicals are advected through the plume, e.g., due to the action of a straining flow, even in the absence of entrainment. As time increases, dilution due to mixing acts to decrease δX_i at local maxima, but increases the fraction of the fluid domain over which δX_i is nonzero. The evolution equation for $\overline{\delta X_i}$ is

$$\frac{d\,\overline{\delta X_i}}{dt} = \overline{f_i\left(X_1^B + \delta X_1, .., X_N^B + \delta X_N\right)} - \overline{f_i\left(X_1^B, .., X_N^B\right)}, i = 1, .., N. \tag{4}$$

Note that there is no explicit dependence on the diffusivity k in this equation although the implicit dependence on mixing will be discussed below. The initial conditions for (4), $\overline{\delta X_i}(0) = \overline{\delta S_i}$, relates the chemical source to the integrated products in the plume at $t = 0$. Note that the integral of δS_i disappears at later times as we are downstream of the source.

[14] An important limit in the behavior of equation (4) is the dilute regime, i.e., when $|\delta X_i| \to 0$ for each species. At large times mixing may result in emissions eventually decaying according to the dilute regime even if those emissions are initially at high concentrations. Because the $|\delta X_i|$ are small in this limit, equation (4) can be linearized so that

$$\frac{d\,\overline{\delta X_i}}{dt} \approx \sum_j A_{ij}\overline{\delta X_j}, \qquad i = 1, .., N. \tag{5}$$

In the case where the dilution is by the constant background atmosphere with concentrations $\mathbf{X^B} = (X_1^B, .., X_N^B)$ the A_{ij} are given by

$$A_{ij} = \left.\frac{\partial f_i}{\partial X_j}\right|_{\mathbf{X^B}}. \tag{6}$$

The A_{ij} can be considered components of an $N \times N$ matrix $\mathcal{A}$. The eigenvectors $\mathbf{R_j}$ of $\mathcal{A}$ (which satisfy $\mathcal{A}\mathbf{R_j} = \lambda_j\mathbf{R_j}$) have been described as "chemical eigenstates" [*Prather*, 1994], and have timescales associated with N corresponding eigenvalues λ_j. These eigenvalues may include complex conjugate pairs, corresponding to modes with an oscillatory component. Throughout this paper it is assumed that all the λ_js have negative real parts, ensuring that the chemistry is stable (nonchaotic).

[15] Equation (5) may be accurate for the chemical evolution in a diluted plume after some time t_1 after which time the general solution be written in terms of the eigenvectors [*Prather*, 1996],

$$\overline{\delta\mathbf{X}}(t - t_1) = \sum_j \alpha_j\mathbf{R_j}\exp\lambda_j(t - t_1) \qquad i = 1, .., N, \tag{7}$$

where α_j are components of the vector α given by $\alpha = \mathcal{R}^{-1}\overline{\delta\mathbf{X}}(t_1)$. Here the matrix $\mathcal{R}$ has components R_{ij} given by the ith component of the eigenvector $\mathbf{R_j}$, and the vector $\delta\mathbf{X} = (\delta X_1, .., \delta X_N)$. The time t_1 will depend on the choice of plume dilution model, the initial concentrations of the emissions and details of the chemistry scheme. In the atmosphere typical choices might be of the order of 0.5 to 5 days.

[16] Equations (4) and (5) provide a method for evaluating the total (time-integrated) perturbation M_i to the atmosphere deriving from each continuous source. Essentially, M_i measures the globally integrated contribution of the source to the atmospheric loading of the ith species.

$$M_i = \int_0^\infty \overline{\delta X_i}(t)\,dt \approx \int_0^{t_1} \overline{\delta X_i}(t)\,dt - \sum_j \frac{\alpha_j(t_1)R_{ij}}{\lambda_j} \qquad i = 1, .., N \tag{8}$$

The second part of the expression for M_i is obtained by assuming decay according to (7) after time t_1, enabling the integral to be evaluated from $t = t_1$ to $t = \infty$. Typically, M_i converges to a constant that is independent of t_1 for sufficiently large t_1, i.e., once the plume becomes dilute. Much of the rest of this paper will be concerned with the extent to which this measure of global contribution depends on the manner in which the emissions from each source are mixed.

2.2. Equivalent Emissions and the Parameterization Scheme

[17] The basis of the suggested parameterization is that individual emission sites δS_i that give rise to unresolved subgrid plumes in a model can be replaced by equivalent emissions δS_i^E that when diluted rapidly (as in a model grid-box) have the same total impact on the global chemistry as

the unresolved plumes. The dilution scenario for the subgrid plumes is assumed known. We calculate equivalent emissions for some idealized plumes in section 4, and the parameterization is tested in a simple plume-box model problem in section 5.

[18] If equivalent emissions are to mimic the effects of subgrid plumes developing from actual emissions sites in a model, then ideally they ought to satisfy the following criteria:

[19] 1. The net chemical products from the equivalent emissions converge to the net products calculated for the subgrid plume on the timescale it takes for the plume to be effectively diluted by background air.

[20] 2. The total atmospheric burden, i.e., the time-integrated amount, of each species resulting from the equivalent emissions is equal to that calculated for the subgrid emissions.

[21] For the purposes of this paper we will assume that when the equivalent emissions are released into the model, instant dilution takes place so that the chemical perturbation decays according to (7) from $t = 0$. In cases where the plume from an emissions site is partially resolved by a model, however, it is possible to modify the following analysis to calculate appropriate equivalent emissions for the partially resolved plume.

[22] The equivalent emissions δS_i^E can be derived from each plume source δS_i as follows. Defining $\overline{\delta X}_i^E(t)$ as the integrated chemicals remaining at time t in the CTM grid-box and denoting as before that remaining in the unresolved plume by $\overline{\delta X}_i(t)$, criteria 1 and 2 above for determining the equivalent emissions may now be written:

[23] 1. The emission convergence criterion becomes $\overline{\delta X}_i^E \rightarrow \overline{\delta X}_i$ at times $t \sim t_1$.

[24] 2. The total mass condition becomes

$$P_i = \int_0^{t_1} \overline{\delta X}_i^E \, dt = \int_0^{t_1} \overline{\delta X}_i dt. \qquad (9)$$

Note that because this integral equality holds up to time t_1, criterion 1 will ensure it holds thereafter. We refer to P_i below as the total plume mass of species i, with $\mathbf{P}$ as the corresponding vector. Criterion 2 essentially amounts to replacing the anomalous chemicals undergoing nonlinear (high-concentration) chemistry in the early stages of the plume with an equal mass of chemicals undergoing linear decay in the dilute regime. Criterion 1 ensures that they converge to the same chemical products.

[25] The most general way criterion 1 can be satisfied is by replacing δS_i at each time t_0 with a grid-box source δS_i^E that takes the form of a series of N emissions at times $t_0 + \tau_j$ with magnitude $\alpha_j \, \mathbf{R_j} \exp \lambda_j(\tau_j - t_1)$. As the equivalent emissions are assumed to be instantaneously diluted and therefore decay with the eigenstate timescales, these emissions will decay according to (5). This ensures that they will be equal to the total plume products at time $t_0 + t_1$, regardless of the choices of the N times τ_j. Note that if δS_i is constant or slowly varying in time then the "time lags" associated with the τ_js are not significant, the τ_js in this case just determine the amplitude of each eigenstate component of δS_i^E. The freedom to choose the τ_js allows the total mass criterion 2 to be satisfied. In terms of the plume mass vector $\mathbf{P}$ above, (9) may be shown to be satisfied if (under the assumption of real λ_j for this example),

$$\tau_j = t_1 + \frac{1}{\lambda_j} \log\left(-\frac{\lambda_j (\mathcal{R}^{-1}\mathbf{P})_j}{\alpha_j} + 1 \right), \qquad j = 1, .., N. \qquad (10)$$

It is easily shown that, provided the plume is in the dilute regime by time t_1, both the τ_j and the magnitudes of the emissions $\alpha_j \mathbf{R_j} \exp \lambda_j(\tau_j - t_1)$ are independent of the choice of t_1. It is also the case that equivalent sources will be equal to actual sources in cases where the source is sufficiently weak (or dispersed) that the initial plume concentrations do not differ greatly from the background. Similarly, the shorter the timescale of dilution in the plume model, the closer the equivalent emissions will be to the actual emissions.

[26] The above calculations are for a time invariant chemistry scheme. Real tropospheric photochemistry, of course, has a strong diurnal cycle which is itself nonlinear. In principle, Floquet theory may be used to calculate chemical eigenstates and eigenvalues for a periodic (i.e., diurnally varying) chemistry. A further underlying assumption of this approach is that the most important eigenmodes do not vary dramatically in structure and timescale as the background state is varied. The extent of temporal variation in background concentrations at an emissions site is likely in practice to determine the accuracy of the equivalents emissions-based parameterization for that site.

3. Simple Models of Tropospheric Chemistry and Plume Dilution

3.1. Tropospheric Chemistry Scheme

[27] The evolution of many long-lived species in tropospheric chemistry is largely determined by reactions with relatively short-lived radical species [*Ehhalt*, 1998]. Among the most important radicals are the HO_x family, comprising the hydroxyl radical OH and the hydroperoxy radical HO_2. At solar zenith angles less than 75°, HO_x concentrations may be considered to be in photochemical steady state, i.e., concentrations can be determined by equating production and loss terms [*Jaegle et al.* 1999]. An important nonlinearity in tropospheric chemistry arises because in the photochemical steady state, HO_x concentrations depend nonlinearly on the concentrations of longer lived precursors, such as O_3, CO, and NO_x. Each of these precursors themselves react with HO_x, so because they influence HO_x concentrations, their rate of production or loss in reactions involving HO_x are nonlinear functions of their concentrations.

[28] For demonstrative purposes we intend to use a simple chemistry scheme to highlight some of the ideas discussed in section 2. The scheme is based on the reactions in Table 2, with details of the steady state approximations used to determine radical concentrations from precursor concentrations described in Appendix A. The intention with this scheme was maintain the correct qualitative relationship between the concentration of each precursor species and its rate of production or loss in reactions involving HO_x. By doing this we intend to correctly model key components of the nonlinearity, and hence the sensitivity to mixing inherent

in tropospheric chemistry. The scheme is defined by the three evolution equations

$$\frac{d[O_3]}{dt} = -\frac{S_{NO}}{1+R_N} + \frac{R_N k_8}{1+R_N}[HO_2][NO_x] - (k_5[OH] + k_2[HO_2] + k_4[H_2O])[O_3] \quad (11)$$

$$\frac{d[CO]}{dt} = S_{CO} - k_1[OH][CO] \quad (12)$$

$$\frac{d[NO_x]}{dt} = S_{NO} - \frac{k_6}{1+R_N}[OH][NO_x] \quad (13)$$

in conjunction with the steady state approximations (A1)–(A3). The system is forced by emissions of NO and CO, of strength S_{NO} and S_{CO} (note also the first "titration" term in the ozone equation). Other parameters include $[H_2O]$, $P(HO_2)$ and $k_X[X]$, which are kept fixed through the experiments described below at values $[H_2O] = 750$ ppmv, $k_X[X] = 5.53 \times 10^{-2}$ s^{-1}, $P(HO_2) = 1.29 \times 10^{-3}$ pptv s^{-1}. This is justified only in order to concentrate on mixing effects due to the other precursor species O_3, NO_x and CO. However, the experiments described below have been repeated with a wide range of $[H_2O]$ and $P(HO_2)$ values, with the qualitative nature of the sensitivity to mixing unchanged. Note, however, that this does not rule out the possibility of mixing sensitivities due to correlations between $[H_2O]$, $P(HO_2)$ and the other precursors.

[29] Several properties of this simple scheme correspond to key features of the tropospheric chemistry system. Perhaps the most important of these is the dependence of the radical concentrations [OH] and $[HO_2]$ as well as the ozone production rate $P(O_3)$ on $[NO_x]$. This is illustrated in Figure 2 for typical midtropospheric conditions. The qualitative features of these curves agree well with those from steady state models that have been verified directly against observations [*Brune et al.*, 1999; *Jaegle et al.*, 1999]. Another property of the scheme is that the effect of increasing [CO] is to reduce [OH], effectively extending the lifetime of CO. Because it captures these important features, we believe that this O_3-CO-NO_x scheme as defined by (11)–(13) will exhibit similar sensitivity to mixing as exists in tropospheric chemistry.

[30] Figure 3 illustrates the structure of the chemical eigenstates of this chemistry scheme, calculated at typical concentrations with reaction rates at 250 K, 500 mbar as in Table 2. This calculation was made using a 3×3 matrix $\mathcal{A}$ equation (6). However, as explained in detail by *Poppe* [1999], to correctly evaluate the partial derivatives in $\mathcal{A}$ it is necessary to include the dependence of [OH] and $[HO_2]$ on their precursors, e.g.,

$$\frac{\partial f_{CO}}{\partial [O_3]} = -\frac{\partial}{\partial [O_3]}([OH][CO]) = -\frac{\partial [OH]}{\partial [O_3]}[CO]. \quad (14)$$

The chemical lifetimes of the individual species and the lifetimes of each eigenstate (eigenmode) are shown alongside the structure. The first eigenstate, the "NO_x mode," has a timescale comparable to the lifetime of NO_x, and is the principle eigenstate excited when NO is released. Following a release of NO, the NO_x mode is strongly excited and decays on the 1.61 day timescale. However, due to the coupling in the chemistry the NO emission also excites the O_3 mode and CO mode. The contributions to these modes decay on the longer timescales (27.23 and 116.78 days respectively). A relatively long-lived increase in O_3 due to the NO emission can be associated with the decay of the O_3 mode. Similarly, an emission of CO excites not only the long-lived "CO mode," but also the two other modes with shorter lifetimes. Note that the CO mode has a longer timescale than the lifetime of CO, because CO acts to decrease OH concentrations in (A2) thereby creating a positive feedback. The O_3 mode has a shorter timescale than the lifetime of O_3 as more HO_x is produced, leading to increased loss of O_3 and also increased loss of NO_x and hence decreased $P(O_3)$.

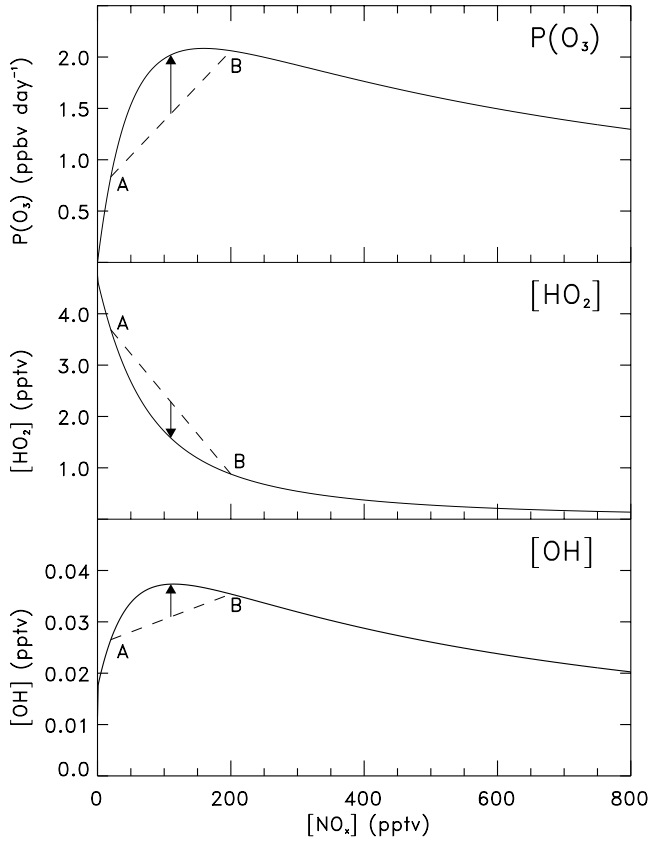

Figure 2. Dependence of $P(O_3)$, $[HO_2]$, and [OH] on $[NO_x]$ in the chemistry scheme defined by equations (13)–(20). Photolysis and reaction rates used are as in Table 2 (250 K, 500 mbar), and we take constant $[O_3] = 50$ ppbv, $[CO] = 100$ ppbv, $k_X[X] = 5.53 \times 10^{-2}$ s^{-1}, $P(HO_2) = 1.29 \times 10^{-3}$ pptv s^{-1}. The dotted lines show the averaged concentrations between two air parcels A and B prior to mixing, and the arrows show the change in average concentrations in the two parcels due to mixing.

3.2. Uniform Concentration Plume Dilution Models

[31] Various suggestions have been made for plume dilution models that account for the combined effects of fluid dynamical stirring, caused by turbulence, and diffusive

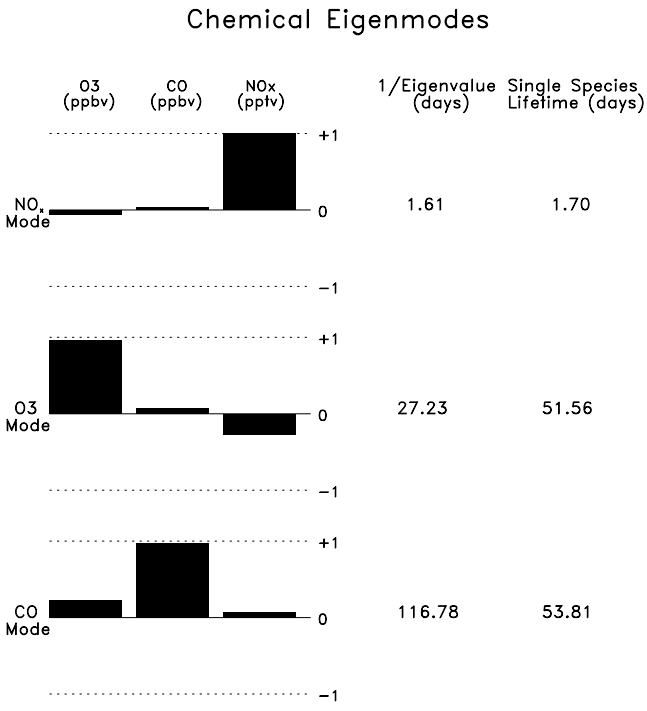

Figure 3. Diagram showing the structure of the chemical eigenmodes (eigenstates) of the O_3-NO_x-CO tropospheric scheme. Any dilute emission can be decomposed into a linear sum of these eigenmodes, and each component of this sum then decays on its characteristic timescale (= 1/eigenvalue shown). The traditional "chemical lifetimes" of NO_x, O_3, and CO in the model are shown for comparative purposes. Source strengths $S_{CO} = 1.66 \times 10^{-5}$ ppbv s^{-1} and $S_{NO} = 1.41 \times 10^{-4}$ pptv s^{-1} were used to obtain equilibrium concentrations in the background state of $[O_3] = 62.28$ ppbv, $[CO] = 96.50$ ppbv, $[NO_x] = 27.62$ pptv.

mixing within the plume [*Konopka*, 1995]. Typically the diffusion operator in (2) is replaced with a stronger anisotropic diffusion and (2) is then solved in a coordinate system perpendicular to the plume axis, assuming that mixing ratios are constant on appropriate time-evolving elliptical surfaces [*Meijer*, 2001; *Vilà-Guerau de Arellano et al.*, 1990]. The above global measure M_i can be easily adapted for use with these models of chemical dispersion. In the interests of simplicity, however, an alternative choice is to use a single-concentration box model to describe the dilution in the plume [*Wild et al.*, 1996; *Poppe et al.*, 1998]. In this model the plume has a uniform anomalous concentration $\delta X_i(t)$ within a volume element $\delta V(t)$ with constant background air ($\delta X_i(t) = 0$) outside of this area. Entrainment of background air causes the volume element $\delta V(t)$ to increase with time since emission, while the concentrations $\delta X_i(t)$ are diluted. The diffusion term in (2) is replaced by $\kappa(t)\delta X_i$ and

$$\delta V(t) = \delta V(0) \exp\left\{ \int_0^t \kappa(t')dt' \right\}. \quad (15)$$

The integrated plume products in equations (4)–(8) are given by

$$\overline{\delta X_i}(t) = \delta X_i(t)\, \delta V(t). \quad (16)$$

We shall use this type of plume box model in section 4 to test the sensitivity to different mixing scenarios of a simple chemistry scheme. To our knowledge there is no widely agreed, observationally verified choice of $\kappa(t)$ appropriate for global-scale polluted plumes [*Brunner et al.*, 1998] of the type we are considering. For this reason we choose instead to investigate a wide range of dilution scenarios as detailed in Table 1. The first scenario of constant dilution rate $\kappa = 1/\tau$ is chosen for its conceptual simplicity. The second scenario of no mixing up to a time τ followed by instantaneous mixing is a crude model of the situation common in chaotic advection flows. In this case pollutants are initially unmixed within filaments with initial width L. These filaments are locally stretched and elongated by the strain component of the large-scale flow at rate Γ. The straining flow reduces the width of the filaments until they reach the diffusive scale $\sqrt{\kappa/\Gamma}$ at time $\tau = (1/\Gamma) \log L\sqrt{\Gamma/\kappa}$. The filament is then mixed into the background on the timescale $1/\Gamma$ which can be much less than τ. The remaining scenarios are those used in previous work and are included for comparative purposes. The "fast" entraining plume scenario of *Wild et al.* [1996] corresponds to a model of an entraining plume in a neutral turbulent boundary layer.

4. Sensitivity to Mixing of a Single Isolated Source and "Equivalent Emissions"

[32] In this section we aim to compare the total perturbation M_i equation (8) to a constant background atmosphere due to a single, constant, continuous chemical source δS_i. The intention is to highlight the dependence of M_i on the details of the mixing of the plume of emitted chemicals with the background atmosphere. For each plume mixing scenario, we then calculate the "equivalent emissions" for the source, that is to say those emissions that when mixed instantly into the background result in the same M_i for each species as the slowly mixed plume. The idea, as described in section 2, is that the emissions in a model with limited resolution, and which therefore cannot

Table 1. Table of Plume Dilution Models Used[a]

	Dilution Rate	Volume Element	Physical Intepretation and References
Dilute	$\kappa(t) = 1/\tau$	$\delta V(t) = \exp\{t/\tau\}$	constant dilution rate
Mix	$\kappa(t) = 0$ for $t < \tau = \infty$ for $t \geq \tau$	$\delta V(t) =$ cons. for $t < \tau = \infty$ for $t \geq \tau$	chaotic advection [*Ottino*, 1989]
Plume fast	$\kappa(t) = 2/(t + \tau)$	$\delta V(t) = (t + \tau)^2$	turbulent entraining plume [*Wild et al.*, 1996]
Plume slow	$\kappa(t) = 1/(t + \tau)$	$\delta V(t) = (t + \tau)$	*Wild et al.* [1996]
Poppe	$\kappa(t) = (1 + (b/a) \exp\{-t/\tau\})^{-1}$	$\delta V(t) = a + b \exp\{t/\tau\}$	fit to observations [*Poppe et al.*, 1998]

[a] $\kappa(t)$ is the rate of entrainment of background air into the plume, and $\delta V(t)$ is the cross-sectional area of the plume. τ is a constant timescale in each case.

resolve the plume, can be replaced by the equivalent emissions. This would have the effect of reducing the systematic error associated with the subgrid chemistry. (The case where the plume is partially resolved in the model can also be dealt with by a modified treatment). Here, for demonstrative purposes, we will concentrate on the idealized chemistry and plume models described in section 3, although there is no barrier in principle to applying the techniques described in section 2 to any plume model or chemistry scheme. To further simplify matters we assume that reaction rates and mixing ratios are constant in the background atmosphere in order that the chemical eigenstates method can be straightforwardly used to evaluate M_i. Also, the background atmosphere is assumed to be an equilibrium solution of (11)–(13), with chemical forcing S_{CO} and S_{NO} representing the effects of in-situ production and remote sources.

[33] The emissions from the isolated source δS_i are then subject to the varying dilution scenarios detailed in Table 1, so that the effect of each dilution scenario can be compared directly. The isolated source is chosen to have total magnitude $\overline{\delta S}_{CO} = 1$ Tg yr^{-1} and $\overline{\delta S}_{NO} = 0.0214$ Tg yr^{-1}. Initially the emissions are assumed to be rapidly diluted (e.g., by boundary layer turbulence) and the local background NO_x and CO concentrations are increased by 10 ppbv and 500 ppbv respectively, as might be typical at an industrial site or site of biomass burning. Titration of ozone, from the instantaneous conversion of some of the NO released to NO_2, causes $[O_3]$ at the source to decrease by $1/(1 + R_N) \times 10$ ppbv.

[34] Figure 4 shows how the total anomalous mass of O_3 (top) and CO (bottom) evolves in the plume from the time of release. In the terms of section 2 the quantities plotted are $\overline{\delta X_i}(t) = \delta X_i(t)\delta V(t)$ for $i \equiv O_3$ and CO. Note that the solid red curve corresponds to instantaneous dilution into the background at time $t = 0$, so that the chemical perturbation decays according to (7) from $t = 0$. The area under these curves is the total perturbation due to a continuous plume (i.e., M_i for $i \equiv O_3$ and CO). Note that the total anomalous mass of each species in the plume decays on the chemical timescales, even though the anomalous concentrations might be very low after just a few days, since mixing ratios in the plumes decay on the dilution timescale.

[35] It is notable from Figure 4 (top) that the peak ozone perturbation for the instantaneously mixed case is, from 2–20 days, many times greater than other more slowly mixed plumes. However, at long times (~100 days) when the main contribution is from the longest-lived eigenstate it is significant that the ozone perturbation for the rapidly mixed case is then smaller than that of the slowly mixed plumes. Because this remaining ozone perturbation is decaying on the timescale of the longest-lived eigenstate (116.78 days) the long-time chemical perturbation contributes significantly to $M_{i\equiv O_3}$ (depending on dilution scenario, between 15% and 70% of the contribution to $M_{i\equiv O_3}$ are due to emissions over 60 days old, see Figure 5). The level of excitation of the longest-lived eigenstates is therefore sensitive to the initial mixing. Previous studies of sensitivity to mixing [*Poppe et al.*, 1998; *Wild et al.*, 1996] have concentrated on differences in the short-time evolution of the ozone perturbation due to mixing. However, they did not address the possibility of significant differences in long-time decay

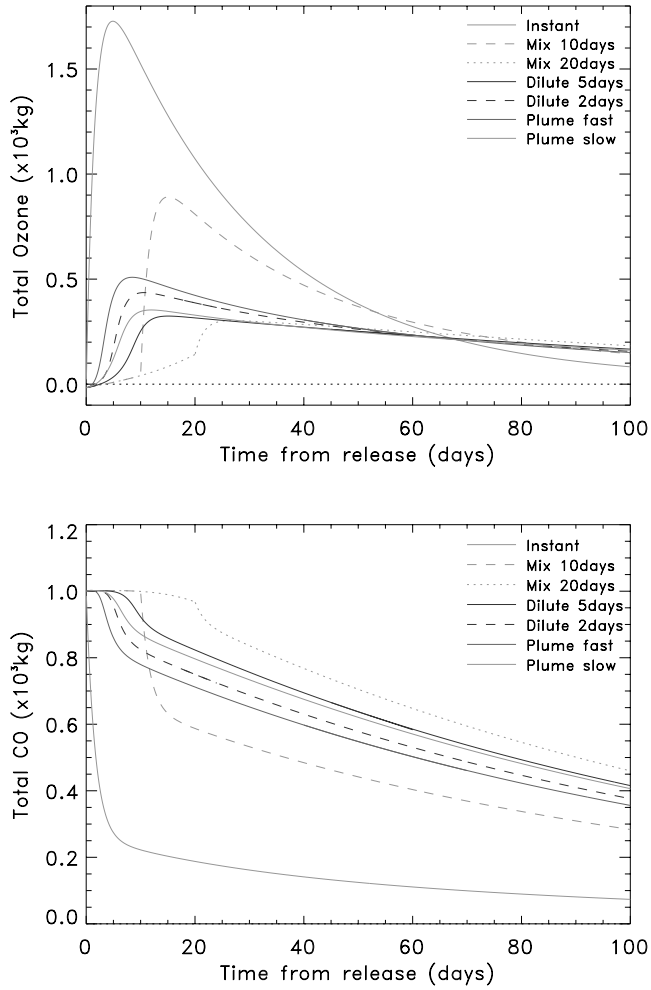

Figure 4. Evolution of total anomalous (top) O_3 and (bottom) CO in each plume from the time of release ($\overline{\delta X_i}(t) = \delta X_i(t)\delta V(t)$ for $i \equiv O_3$, CO). The different curves correspond to the different mixing scenarios described in Table 1, with the timescale parameter τ as labeled in the inset. At early stages the evolution is determined explicitly by numerically integrating (2) and at later times this is matched to the "dilute" solution (7). See color version of this figure at back of this issue.

substantially changing the overall global atmospheric sensitivity to the initial mixing.

[36] Figure 5a (black points) shows the total perturbations M_i for the same chemical source plotted as points on an O_3 versus CO scatterplot. The solid square corresponds to the instantaneous mixing scenario. The unfilled squares correspond to the "mix" scenario in which the plume remains unmixed for 1, 2, 5, 10 and 20 days respectively (in the direction of the "increasing τ" arrow) and is then rapidly mixed into the background. Similarly the stars apply to the constant dilution scenario (with τ = 0.25, 0.5, 1, 2, and 5 days), the filled triangle to the turbulent entraining plume case with τ = 1 day, and the unfilled triangle to the slow dilution case of *Wild et al.* [1996] also with τ = 1 day.

[37] Looking first at the black points in Figure 5a, it is clear that the global effect of the emissions depends significantly on the way in which they are diluted. Rapidly diluted

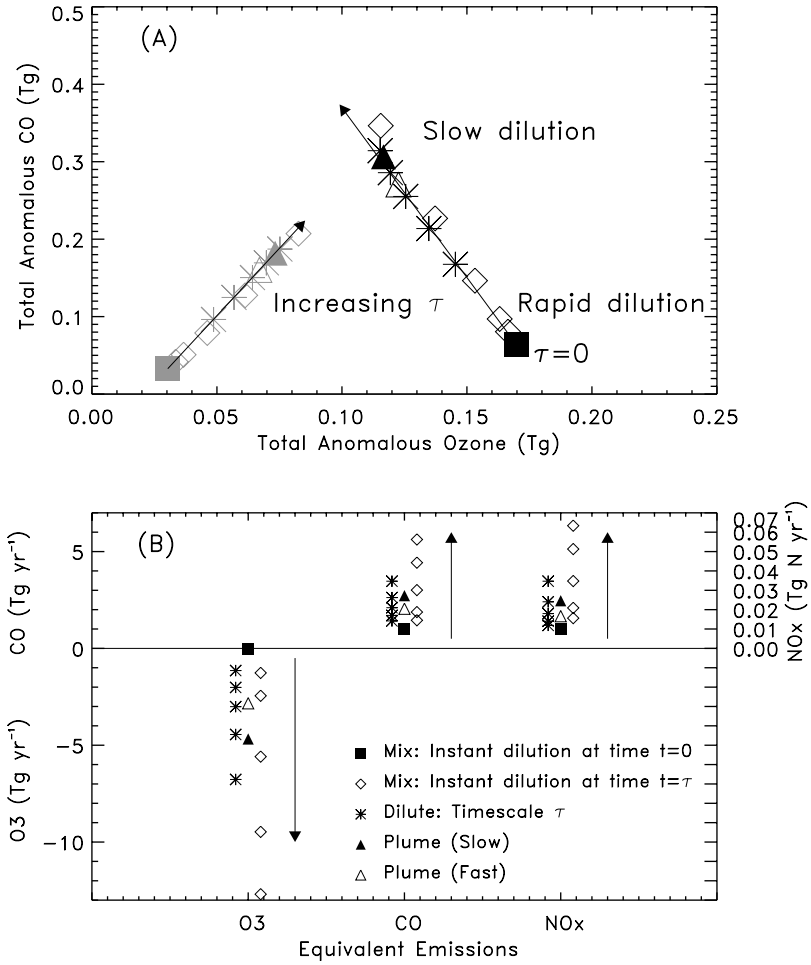

Figure 5. (a) The black points show the variation in M_i (equation (8), $i = O_3$, CO) with mixing scenario and timescale for a continuous isolated source of strength $\overline{\delta S_{NO}} = 0.0214$ Tg N yr^{-1} and $\overline{\delta S_{CO}} = 1$ Tg yr^{-1}, with initial concentrations 10 ppbv NO_x and 500 ppbv CO at the plume bases. The case of instantaneous mixing is shown by the solid square, with the other scenarios as in the key (with timescales τ as described in the text). The grey points show the contribution to M_i from emissions older than 60 days, illustrating how the long-time decay of the chemical perturbation depends on the initial mixing scenario of the plume. (b) The equivalent emissions of O_3, CO, and NO_x for each of the plumes. The arrows denote the direction of increasing τ.

emissions result in greater excess ozone produced, compared with those slowly diluted in entraining plumes or in plumes isolated for a prolonged period. Also, over four times as much excess CO enters the atmosphere in the most slowly diluted plume (the τ = 20 days isolated plume) compared with the instantaneous dilution case. The excess CO is reduced for rapidly diluted plumes because there is a greater increase in global mean OH levels for rapidly mixed emissions compared with slowly mixed emissions. It is also noticeable from Figure 5 that most of the points lie approximately along a single straight line, so that quite different dilution scenarios have nearly identical global effects (e.g., the cases with no mixing followed by instant dilution after 10 days and the case with constant dilution with $\tau = 1$ day^{-1}). Very similar results were obtained using different background concentrations, with points falling on the CO:O_3 scatterplot very close to the straight line sketched by the red points. (The different background concentrations used were obtained by varying first S_{NO}, then S_{CO} by ±20%.) Qualitatively similar results were also obtained when the chemistry parameters were adjusted to settings appropriate to the boundary layer, by setting pressure to 1000 hPa, temperature to 285K and quadrupling the source of HO_x.

[38] The grey points in Figure 5a illustrate the contribution to M_i from emissions over 60 days old. For each plume these long-diluted emissions make a considerable contribution to M_i. This figure therefore illustrates the importance of considering long-time decay when evaluating sensitivity to mixing. The chemistry proceeds more slowly in the slowly mixed plumes, and older emissions make a much greater contribution to M_i compared with the rapidly mixed cases. The increased contribution from older emissions partially compensates for the much lower amounts of ozone produced shortly after the time of emission in the slowly mixed plumes.

[39] Figure 5b shows the "equivalent emissions" calculated for each plume mixing scenario. These are the

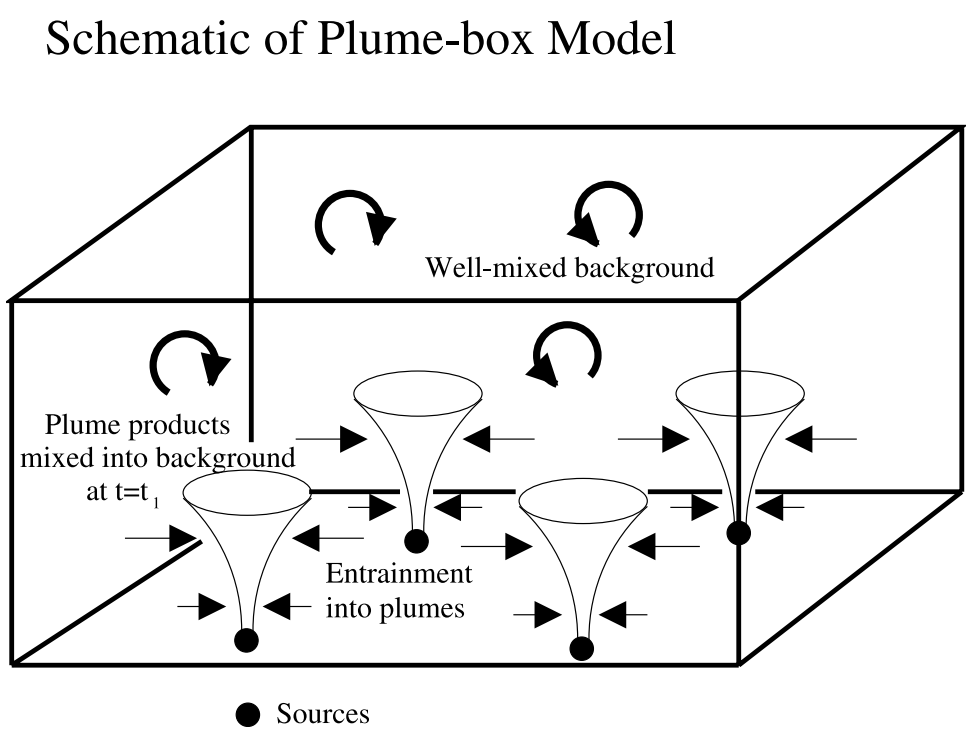

Figure 6. Schematic of the plume-box model described in section 5. Emissions from the sources evolve in (entraining) plumes until time t_1 when they are mixed uniformly into the background. The background is allowed to evolve as a standard box model with the chemical source provided by the products from the (dilute) plumes at t_1. The domain volume V is set to 2.8×10^{18} m^3 based on a free tropospheric mass of 4×10^{18} kg and a typical density of 0.7 kg m^{-3}. The total sources representing both anthropogenic and natural emissions are taken to be $S_{NO} = 13.07 \times 10^9$ kg N yr^{-1} and $S_{CO} = 2245 \times 10^9$ kg CO yr^{-1} and these are introduced so that the concentrations at the base of the plumes are 4.17 ppbv NO_x and 368 ppbv CO. This corresponds to a initial choice of "volume fraction" for the plumes of $\delta V^P(0) = 5 \times 10^{-8} V s^{-1}$, chosen in order that concentrations at the base of the plumes were representative of urban or industrial areas.

emissions that when diluted instantly into the background atmosphere result in the same global perturbation of each species (i.e., the same M_i) as the corresponding plume. For fast mixing scenarios the equivalent emissions are close to the actual emissions. For slower mixing scenarios, however, in which chemistry proceeds at high concentrations in the plume for a prolonged period before dilution, the equivalent emissions deviate significantly from the actual emissions. As the rate of mixing is reduced, the equivalent emission includes more CO and more NO_x and also contains a sink of O_3. The artificial O_3 sink and artificial extra contributions to the NO_x and CO sources by design will have the same net effect on the background atmosphere to the processing of the chemicals in the plume at high concentrations.

5. Testing the Parameterization in a Global Box Model Forced by Plumes

[40] In this section we demonstrate the utility of the parameterization in a simple box model that is forced by entraining plumes such as those described in section 3.2 above. The object is to show in a simple framework that the systematic error induced in a box model when plume-like chemical sources are replaced by a uniform source can be reduced or eliminated by using equivalent emissions in place of the actual emissions. The problem is intended as an idealized model problem that is essentially analogous to the problem of reducing the systematic error in chemistry transport models due to diluting subgrid sources too rapidly in model grid-boxes. By comparing the mean equilibrium concentrations in the box model when it is uniformly forced by equivalent emissions, to the equilibrium concentrations when it is forced by the actual emissions in entraining plumes, we can determine the extent to which the equivalent emissions can efficiently substitute for the entraining plumes. It is important to emphasize that no a priori information about the mean equilibrium state in the plume-box model is used to obtain the equivalent emissions, instead these are obtained following the recipe in section 2.

[41] The plume-box model is illustrated schematically in Figure 6. As before, the model idealizations include constant photolysis and reaction rates and constant mixing ratios outside of the plumes. These idealizations are not necessary in order to apply the parameterization, but they serve to make a simple demonstration of the parameterization more straightforward. In the rapid dilution limit for each plume the model is equivalent to a standard chemical box model, which is assumed to be well-mixed everywhere.

If the model is forced by identical entraining plumes as illustrated, and after time t_1 from emission the contents of these plumes are mixed uniformly into the background, then the background concentrations X_i^B satisfy

$$\frac{dX_i^B}{dt} = \frac{\delta V^P(t_1)}{V - V^P(t_1)}\delta X_i^P(t_1) + f_i\left(X_1^B, .., X_N^B\right) \qquad i = 1, .., N. \tag{17}$$

Here $\delta X_i^P(t)$ are the anomalous plume concentrations at time t after emission and these satisfy (2). The total volume element summed over each plume at this time is given by $\delta V^P(t)$, satisfying (15). Equations (17) and (2) are therefore coupled in this formulation as X_i^B influences the chemistry within the plumes in equation (2). The total volume occupied by the plumes is defined by

$$V^P(t_1) = \int_0^{t_1} \delta V^P(t)dt. \tag{18}$$

Steady states solutions of equation (17) are found iteratively by repeated integration of (2) with X_i^B updated after each iteration. (Other technical details and parameter values used in the integration of equation (17) are described in the Figure 6 caption.)

[42] All the emissions in our plume-box model are assumed to take place at the base of point-like plumes as in Figure 6. For each mixing scenario background concentrations the model is integrated until the background concentrations reach equilibrium with the sources from the plumes. If the emissions in the plume-box model are fixed, the resulting equilibrium state depends only on the mixing scenario for each identical plume, which we vary as in section 4. From section 4 we know that the more rapidly plumes are mixed, the more total O_3 and less total CO will be generated in the model atmosphere. We therefore expect the box model to reach an equilibrium state with higher mean O_3 and lower mean CO for rapidly mixed plumes. To confirm this result the resulting model equilibrium states are best compared using the mean concentrations X_i^M integrated over the box. These are given by

$$X_i^M = \left(V - V^P\right)X_i^B + \int_0^{t_1} \delta V(t)\,\delta X_i^P\, dt. \tag{19}$$

The X_i^M are found to be very insensitive to the choice of t_1 (the dilution time of the plumes) provided that it is chosen to be sufficiently large that the plumes are dilute in the sense of section 2.

[43] Figure 7 (red points) shows plots of $\mathbf{X^M} = ([O_3], [CO], [NO_x])$ in the steady states obtained for each different mixing scenario. The difference between Figures 7a and 7b is that for Figure 7a only 20% of the total chemical source is assumed to be plume-like, the remaining source is taken to be uniformly distributed throughout the box. For Figure 7b, by contrast 100% of the chemical source is concentrated in the plumes. As expected fast mixing scenarios result in mean states with lower CO (and NO_x) and higher O_3 compared with slower mixing scenarios. For example in Figure 7b mean CO concentrations increase from 92 ppbv for the instantaneous mixing case to 342 ppbv for the unrealistic "Dilute, τ = 5 days" scenario.

[44] The parameterization technique is tested as follows. For each plume mixing scenario, the plume sources are replaced by a uniform source of equivalent emissions, so that our model is once again a standard box model. The equivalent emissions are derived as described in sections 2 and 4, using the mean state from the instantaneous mixing case as an appropriate background state. Note that no information about $\mathbf{X^M}$ is required to derive the equivalent emissions. If the parameterization is accurate the equilibrium state in the standard box model forced by the equivalent emissions will be close to the mean state of the plume-box model forced by the actual emissions. Figure 7 (blue points) shows the equilibrium states obtained when the standard box model is forced by the appropriate equivalent emissions. The parameterization by equivalent emissions is found to be accurate for all mixing scenarios in Figure 7a, where only 20% of the total source is in the plumes (the blue and red points overlap for each type of plume). The mean equilibrium concentrations of O_3, CO and NO_x are therefore well-reproduced in the standard box model by the parameterized equivalent emissions. The parameterization becomes inaccurate for the slower mixing scenarios shown in Figure 7b (100% source in plumes). This is because one of the assumptions behind the parameterization (see section 2) is that the background state used to calculate the equivalent emissions does not differ dramatically from the actual background state that the parameterization aims to reproduce. In the slow mixing scenarios shown in Figure 7b, however, CO concentrations are over double those in the instantaneous mixing case. The parameterization fails only when the equilibrium state of the chemical system forced by resolved plumes is radically different from the equilibrium state when emissions from the same sources are rapidly mixed.

6. Summary and Conclusions

[45] In this paper an integrated framework was introduced that allows the sensitivity of global tropospheric chemistry to the mixing of emissions to be quantified. The framework is based on dividing the decay of emissions into two stages, a first stage in which the decay is nonlinear, and a later "dilute" stage when the decay is determined by the timescales of the chemical eigenstates [*Prather*, 1994, 1996]. Unlike previous studies of sensitivity to mixing [*Chatfield and Delaney*, 1990; *Poppe et al.*, 1998; *Liang and Jacobson*, 2000], this framework was capable of resolving the how the long-time or "indirect" effects of emissions [*Wild et al.*, 2001] depend upon their mixing history at much earlier times. Consideration of the long-time behavior is essential if even a qualitative relationship between global equilibrium concentrations of chemical species and the mixing of chemical emissions from continuous sources is to be understood.

[46] Next, a simple tropospheric photochemistry scheme combined with various plume dilution models was used to demonstrate the extent of sensitivity to mixing viewed through this framework. As in previous work [*Sillman et al.*, 1990; *Wild et al.*, 1996] the more rapidly a plume of NO_x and CO emissions was mixed into the background atmosphere, the more O_3 was found to be produced at early times, and the more CO was destroyed due to increased

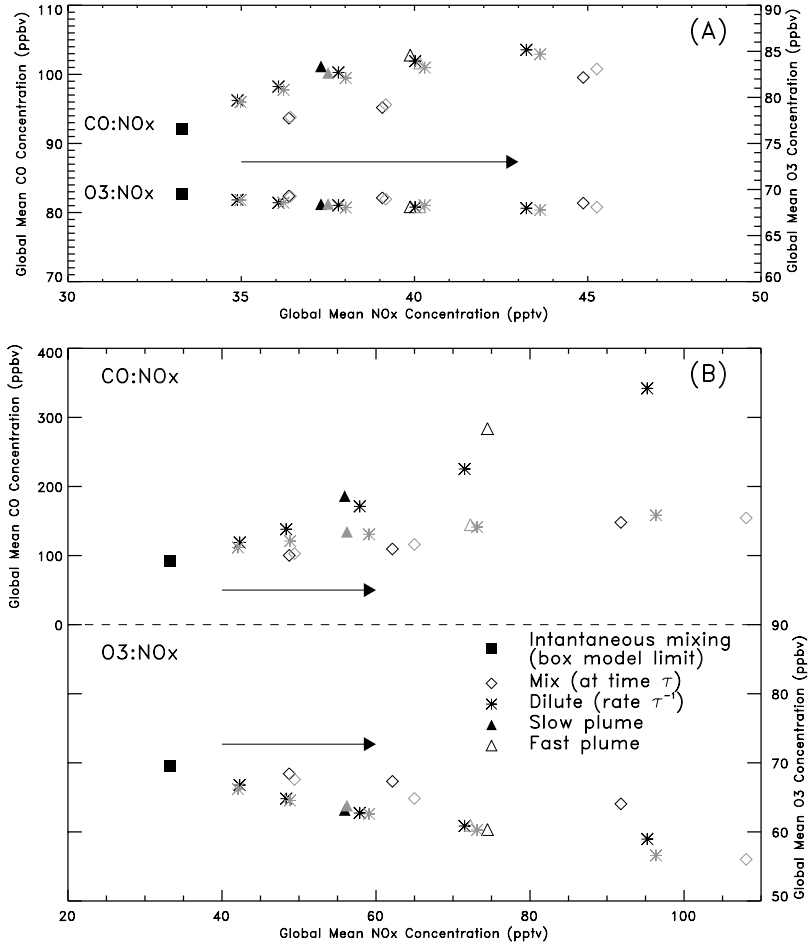

Figure 7. Mean equilibrium concentrations from the plume-box model (red points), and from the standard box model forced using the equivalent emissions (blue points), plotted as O_3:NO_x and CO:NO_x scatterplots. Sources are held constant (see text) and the mixing scenario varied as in Figure 5. The arrows denote the direction of increasing τ (slower mixing). For the "dilute" scenario τ = 0.25, 0.5, 1, 2 and 5 days. For the "mix" scenario τ = 1, 2, and 5 days. Figure 7a corresponds to the case with 20% of the source for the plume-box model in the plumes with the remaining 80% uniformly distributed. Figure 7b corresponds to the case with 100% of the source for the plume-box model in the plumes. See color version of this figure at back of this issue.

production of OH. At long times, however, it was notable that the global O_3 perturbation for those plumes that were initially rapidly diluted was substantially smaller than for those that had been slowly diluted. The long-time behavior therefore partially compensates the slowly mixed sources for not producing as much O_3 at early times. This compensation effect has a significant impact on the sensitivity of global equilibrium concentrations to changes in the mixing of emissions.

[47] One of the main objectives behind examining sensitivity to mixing in an integrated framework was to illustrate that the same concepts can be used in the development of an "equivalent emissions"-based parameterization of subgrid-scale plumes for use in models. The equivalent emissions are designed to have the same global impact when rapidly diluted (as in a model grid-box) as the original emissions have when diluted in a realistic subgrid plume. Equivalent emissions therefore not only converge in time toward the same chemical perturbation as the original plume but also result in the same time-integrated anomaly for each species. Owing to these properties, when equivalent emissions are used to force a box model as described in section 5, they result in a near identical mean equilibrium state as when the model was forced by the corresponding entraining plumes (see Figure 7). The limit on the effectiveness of the parameterization arrives only when the change in mixing scenario of the emissions causes such a substantial nonlinear change in the state of the background atmosphere that the underlying chemical eigenstates are significantly altered.

[48] In order for the parameterization to be developed to the point where it could be used directly in a global model, thorough testing of its numerical robustness under the condition of a realistically varying background remains necessary. Additionally, the theory described in this paper must be extended to a spatially and temporally varying photochemistry. In fact, spatial variation of the photochemistry (e.g., with latitude) will not cause inaccuracy when the

Table 2. Table of Reactions[a]

	Reaction	Reaction Rate at 250 K and 500 mbar	Reaction Rate at 260 K and 750 mbar
R1	$CO + OH + O_2 \rightarrow CO_2 + HO_2$	$k_1 = 1.95 \times 10^{-13}$	2.18×10^{-13}
R2	$O_3 + HO_2 + 2\ O_2 \rightarrow OH$	$k_2 = 1.27 \times 10^{-15}$	1.39×10^{-15}
R3	$O_3 + NO + O_2 \rightarrow NO_2$	$k_3 = 7.50 \times 10^{-15}$	9.27×10^{-15}
R4	$O(^1D) + H_2O \rightarrow 2OH + O_2$	$k_4 = 2.2 \times 10^{-10}$	2.2×10^{-10}
R4b[b]	$O(^1D) + M \rightarrow O + M$	$k_{4b} = 3.06 \times 10^{-11}$	3.02×10^{-11}
R5	$O_3 + OH \rightarrow O_2 + HO_2$	$k_5 = 3.48 \times 10^{-14}$	4.06×10^{-14}
R6	$NO_2 + OH + M \rightarrow HNO_3$	$k_6 = 1.18 \times 10^{-11}$	1.33×10^{-11}
R7	$HO_2 + HO_2(+M) \rightarrow H_2O_2 + O_2$	$k_7 = 3.78 \times 10^{-12}$	3.85×10^{-12}
R8	$HO_2 + NO \rightarrow OH + NO_2$	$k_8 = 9.66 \times 10^{-12}$	9.31×10^{-12}
R9	$OH + HO_2 \rightarrow H_2O + O_2$	$k_9 = 1.30 \times 10^{-10}$	1.26×10^{-10}
R10[c]	$HO_2 + NO_2 + M \rightarrow HNO_4$	$k_{10} = 1.24 \times 10^{-12}$	1.40×10^{-12}
R11	$NO_2 + h\nu + NO + O_3$	$J_1 = 7.00 \times 10^{-3}$	7.00×10^{-3}
R12	$O_3 + h\nu \rightarrow O(^1D) + O_2$	$J_2 = 1.13 \times 10^{-5}$	1.13×10^{-5}

[a]The rates given for (R1)–(R10) are bimolecular reaction rates in cm^3s^{-1}. For the trimolecular reactions, equivalent rates are given with air density calculated from temperature and pressure. The photolysis rates in (R11) and (R12) are in units s^{-1}.
[b]The constant k_4^* in equation (A4) is given by $k_4^* = k_4/(k_{4b}\,[M] + k_4\,[H_2O])$.
[c]In reaction R10 it is assumed that the product HNO_4 is re-photolyzed or reacts with OH, recovering the NO_x molecule with the loss on average of $1 \times HO_x$.

plume becomes dilute on a faster timescale than that on which significant advection takes place. Floquet theory can be used to define equivalent chemical eigenstates and timescales for a time periodic (i.e., diurnally varying) photochemistry. Because of these considerations, and the ever increasing resolution of chemical transport models, it is envisaged that this parameterization will prove most useful in evaluating and reducing systematic error in coarse resolution chemistry-climate models or two-dimensional models, rather than being used universally. Another useful area of application will be to parameterize those emission plumes that have scales below even the finest current CTM grid-scale, and are diluted predictably, and rapidly compared to the transport timescale, into a relatively constant background. Clear examples of such emission plumes are aircraft and ship plumes. Unlike previously suggested schemes [*Sillman et al.*, 1990; *Jacob et al.*, 1993] this suggested parameterization has the advantage that its costs are entirely off line, and unlike previous schemes suggested for aircraft plumes [*Kraabøl et al.*, 2000; *Meijer*, 2001] the equivalent emissions are determined objectively, and it is not necessary for some chemical products from each subgrid plume to be arbitrarily discarded from integration in the model.

Appendix A: Details of the Photochemical Steady State Scheme

[49] To derive suitable steady state expressions from the reactions in Table 2, we first assume that partitioning between NO and NO_2 in the NO_x family is close to a photochemical steady state. Hence we make the approximation that reactions R3 and R11 recycle the NO_x family between NO and NO_2 rapidly compared with the other reactions involving NO_x. This means that the ratio $R_N = [NO]/[NO_2]$ may be expressed

$$R_N = \frac{[NO]}{[NO_2]} = \frac{J_{11}}{k_3[O_3]}, \tag{A1}$$

[*Brunner et al.*, 1998]. Note that this approximation inevitably breaks down at low O_3 concentrations when reactions R6 and R8 become important. The titration of O_3 due to the conversion of emitted NO into NO_2 is treated as a separate, instantaneous, process in equation (11).

[50] Similarly the ratio $R_H = [OH]/[HO_2]$ is assumed to be determined by rapid recycling between OH and HO_2 in reactions R1, R2, R5 and R8. If we make the approximation that these reactions are much faster than the source/sink reactions for HO_x (reactions R4, R6, R7, R9, and R10) we can then write

$$R_H = \frac{[OH]}{[HO_2]} = \frac{k_2[O_3] + \dfrac{k_8 R_N}{1 + R_N}[NO_x]}{k_5[O_3] + k_1[CO] + k_X[X]}. \tag{A2}$$

Here the $k_X[X]$ term represents interconversion in reactions with hydrocarbons, such as methane, that are not explicitly modeled here. Similar steady state expressions for R_H have been presented in the literature [*Brune et al.*, 1998; *Lanzendorf et al.*, 2001; *Poppe et al.*, 1995].

[51] By considering the steady state expression for the HO_x budget in reactions R4, R6, R7, R9, and R10, after some manipulation the following expression can be obtained:

$$[HO_2] = \left(R_1^2[NO_x]^2 + \frac{P(HO_x)}{2(R_H k_9 + k_7)}\right)^{\frac{1}{2}} - R_1[NO_x], \tag{A3}$$

where the ratio $R_1 = (k_6 R_H + k_{10})/(4(1 + R_N)(R_H k_9 + k_7))$ and the production rate of HO_x is given by

$$P(HO_x) = 2J_2 k_4^*[O_3][H_2O] + P(HO_2). \tag{A4}$$

The first term in the expression for $P(HO_x)$ corresponds to OH production (see Table 2 caption for the definition of k_4^*) in R12 + R4, and the second to a constant HO_2 production, corresponding to sources from the oxidation of species such as formaldehyde and acetone which we do not consider explicitly. Similar expressions for $[HO_2]$ concentration are given by *Faloona et al.* [2000] and *Poppe et al.* [1995] and

similar principles are used by *Kleinman et al.* [2001] in deriving an expression for $[HO_2]$ in a model including the effects of volatile organic compounds. One of the motivations in deriving the expressions (A1)–(A3) for R_N, R_H, and $[HO_2]$ was to illustrate explicit dependencies on precursor concentrations. This is why we have avoided using [NO] and $[NO_2]$ in the above expressions as taken individually they are not conserved under mixing processes, whereas the longer lived family NO_x is conserved. More accurate expressions, including state-of-the-art photochemical steady state models [*Jaegle et al.*, 2000], are generally solved by iterative procedures, obscuring the explicit dependence of the radical concentrations on their precursor concentrations.

[52] **Acknowledgments.** The author was supported by NERC Fellowship NER/I/S/1999/00137. Thanks to Slimane Bekki, Richard Crowther, Kathy Law, and Fiona O'Connor for helpful comments on an earlier version.

References

Brune, W. H., et al., Airborne in situ OH and HO2 observations in the cloud-free troposphere and lower stratosphere during SUCCESS, *Geophys. Res. Lett.*, *25*, 1701–1704, 1998.

Brune, W. H., et al., OH and HO2 chemistry in the north Atlantic free troposphere, *Geophys. Res. Lett.*, *26*, 3077–3080, 1999.

Brunner, D., J. Staehelin, and D. Jeker, Large-scale nitrogen oxide plumes in the tropopause region and implications for ozone, *Science*, *282*, 1305–1309, 1998.

Chatfield, R. B., and A. C. Delaney, Convection links biomass burning to increased tropical ozone: However, Models will tend to overpredict O_3, *J. Geophys. Res.*, *95*, 18,473–18,488, 1990.

Eduoard, S., B. Legras, and V. Zeitlin, The effect of dynamical mixing in a simple model of the ozone hole, *J. Geophys. Res.*, *101*, 16,711–16,788, 1996a.

Eduoard, S., B. Legras, F. Lefèvre, and R. Eymard, The effect of mixing on ozone depletion in the Arctic, *Nature*, *384*, 444–447, 1996b.

Ehhalt, D. H., Atmospheric chemistry: Radical ideas, *Science*, *279*, 1002–1003, 1998.

Esler, J. G., D. G. H. Tan, P. H. Haynes, M. J. Evans, K. S. Law, P. H. Plantevin, and J. A. Pyle, Stratosphere-troposphere exchange: Chemical sensitivity to mixing, *J. Geophys. Res.*, *106*, 4717–4731, 2001.

Faloona, I., et al., Observations of HOx and its relationship with NOx in the upper troposphere during SONEX, *J. Geophys. Res.*, *105*, 3771–3783, 2000.

Hess, P. G., and S. Madronich, Tropospheric chemical oscillations, *J. Geophys. Res.*, *102*, 15,949–15,965, 1997.

Jacob, D. J., et al., Simulation of summertime ozone over North America, *J. Geophys. Res.*, *98*, 14,797–14,816, 1993.

Jaegle, L., et al., Ozone production in the upper troposphere and the influence of aircraft during SONEX: Approach of NOx-saturated conditions, *Geophys. Res. Lett.*, *26*, 3081–3084, 1999.

Jaegle, L., et al., Photochemistry of HOx in the upper troposphere at northern midlatitudes, *J. Geophys. Res.*, *105*, 3877–3892, 2000.

Kleinman, L. I., P. H. Daum, Y.-N. Lee, L. J. Nunnermacker, S. R. Springston, J. Weinstein-Lloyd, and J. Rudolph, Sensitivity of ozone production rate to ozone precursors, *Geophys. Res. Lett.*, *28*, 2903–2906, 2001.

Kley, D., Tropospheric chemistry and transport, *Science*, *276*, 1043–1045, 1997.

Konopka, P., Analytic Gaussian solutions for anisotropic diffusion in a linear shear flow, *J. Non Equilib. Thermodyn.*, *20*, 78–91, 1995.

Kraabøl, A. G., F. Flatøy, and F. Stordal, Impact of NO_x emissions from subsonic aircraft: Inclusion of plume processes in a three-dimensional model covering Europe, North America and the North Atlantic, *J. Geophys. Res.*, *105*, 3573–3582, 2000.

Lanzendorf, E. J., T. F. Hanisco, P. O. Wennberg, R. C. Cohen, R. M. Stimpfle, and J. G. Anderson, Comparing atmospheric [HO2]/[OH] to modeled [HO2]/[OH]: Identifying discrepancies with reaction rates, *Geophys. Res. Lett.*, *28*, 967–970, 2001.

Liang, J., and M. Z. Jacobson, Effects of subgrid segregation on ozone production efficiency in a chemical model, *Atmos. Environ.*, *34*, 2975–2982, 2000.

Lin, X., M. Trainer, and S. C. Liu, On the nonlinearity of tropospheric ozone production, *J. Geophys. Res.*, *93*, 15,879–15,888, 1988.

Meijer, E. W., Modelling the impact of subsonic aviation on the composition of the atmosphere, Ph.D. thesis, Univ. of Eindhoven, Eindhoven, Netherlands, 2001.

Neufeld, Z., C. Lopez, and P. H. Haynes, Smooth-filamental transition of active tracer fields stirred by chaotic advection, *Phys. Rev. Lett.*, *82*, 2606–2609, 1999.

Ottino, J. M., *The Kinematics of Mixing: Stretching, Chaos, and Transport*, 364 pp., Cambridge Univ. Press, New York, 1989.

Poppe, D., Time constant analysis of tropospheric gas-phase chemistry, *Phys. Chem. Chem. Phys.*, *1*, 5417–5422, 1999.

Poppe, D., J. Zimmermann, and H. P. Dorn, Field data and model calculations for the hydroxyl radical, *J. Atmos. Sci.*, *52*, 3402–3407, 1995.

Poppe, D., R. Koppmann, and J. Rudolph, Ozone formation in biomass burning plumes: Influence of atmospheric dilution, *Geophys. Res. Lett.*, *25*, 3823–3826, 1998.

Prather, M. J., Lifetimes and eigenstates in atmospheric chemistry, *Geophys. Res. Lett.*, *21*, 801–804, 1994.

Prather, M. J., Time scales in atmospheric chemistry: Theory, GWP's for CH_4 and CO, and runaway growth, *Geophys. Res. Lett.*, *23*, 2597–2600, 1996.

Pyle, J. A., and A. M. Zavody, The modelling problems associated with spatial averaging, *Q. J. R. Meteorol. Soc.*, *116*, 753–766, 1990.

Sillman, S., J. A. Logan, and S. C. Wolfsy, A regional scale model for ozone in the United States with a subgrid representation of urban and power plant plumes, *J. Geophys. Res.*, *95*, 5731–5748, 1990.

Tan, D. G. H., P. H. Haynes, A. R. MacKenzie, and J. A. Pyle, Effects of fluid-dynamical stirring and mixing on the deactivation of stratospheric chlorine, *J. Geophys. Res.*, *103*, 1585–1605, 1998.

Vilà-Guerau de Arellano, J., A. M. Talmon, and P. H. J. Builtjes, A chemically reactive plume model for the NO-NO_2-O_3 system, *Atmos. Environ.*, *24*, 2237–2246, 1990.

Wild, O., K. S. Law, D. S. McKenna, B. J. Bandy, S. A. Penkett, and J. A. Pyle, Photochemical trajectory modeling studies of the North Atlantic region during August 1993, *J. Geophys. Res.*, *101*, 29,269–29,288, 1996.

Wild, O., M. J. Prather, and H. Akimoto, Indirect long-term global cooling from NOx emissions, *Geophys. Res. Lett.*, *28*, 1719–1722, 2001.

J. G. Esler, Department of Mathematics, University College London, Gower Street, London WC1E 6BT, UK. (gavin@math.ucl.ac.uk)

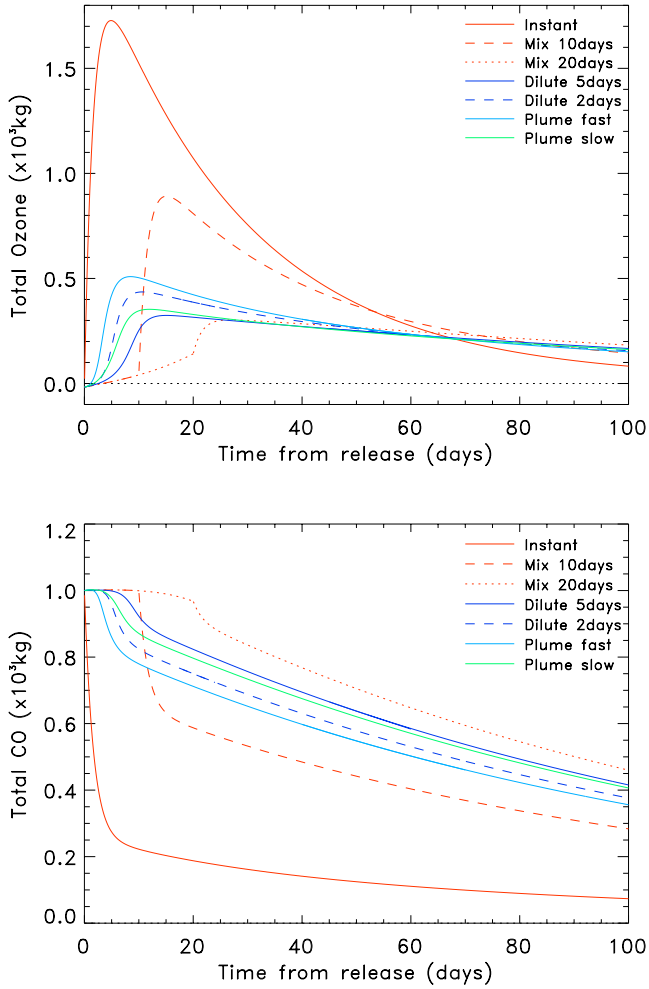

Figure 4. Evolution of total anomalous (top) O_3 and (bottom) CO in each plume from the time of release ($\overline{\delta X_i}(t) = \delta X_i(t)\delta V(t)$ for $i \equiv O_3$, CO). The different curves correspond to the different mixing scenarios described in Table 1, with the timescale parameter τ as labeled in the inset. At early stages the evolution is determined explicitly by numerically integrating (2) and at later times this is matched to the "dilute" solution (7).

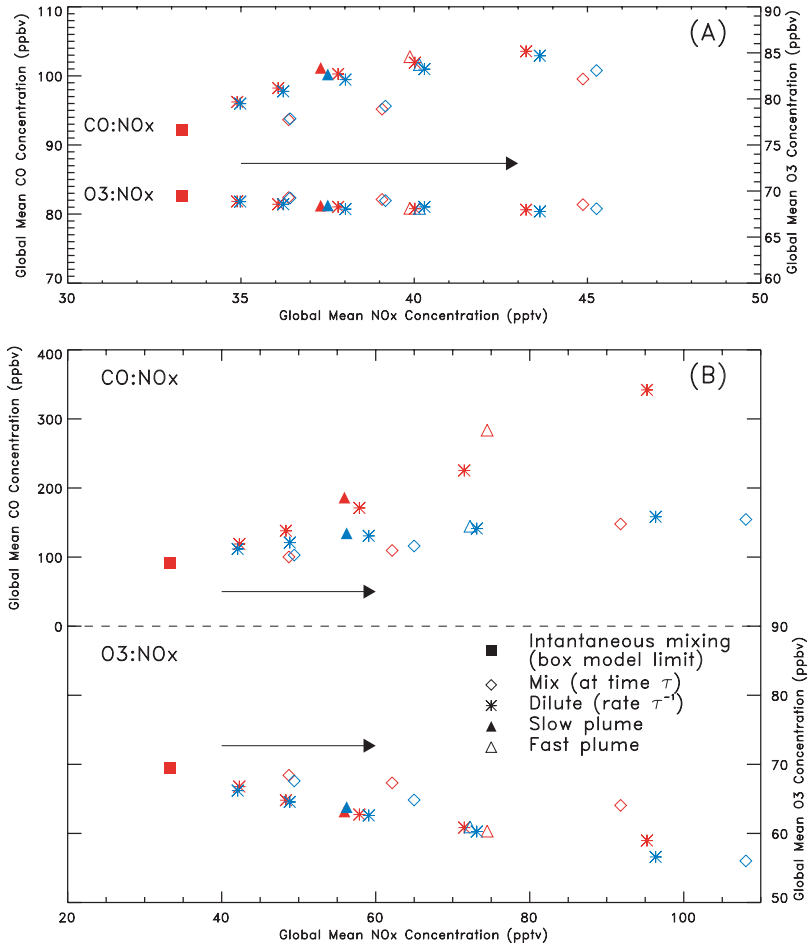

Figure 7. Mean equilibrium concentrations from the plume-box model (red points), and from the standard box model forced using the equivalent emissions (blue points), plotted as O_3:NO_x and CO:NO_x scatterplots. Sources are held constant (see text) and the mixing scenario varied as in Figure 5. The arrows denote the direction of increasing τ (slower mixing). For the "dilute" scenario τ = 0.25, 0.5, 1, 2 and 5 days. For the "mix" scenario τ = 1, 2, and 5 days. Figure 7a corresponds to the case with 20% of the source for the plume-box model in the plumes with the remaining 80% uniformly distributed. Figure 7b corresponds to the case with 100% of the source for the plume-box model in the plumes.